Solid State Science and Technology, Vol. 33, No. 2 (2025) 161-170
https://doi.org/10.66514/ssst332-149-160

Effect of Oxygen Flow During Sintering on the Structural, Superconducting and Microstructural Properties of $YBa_2Cu_3O_{7-\delta}$

Nur Athirah Che Dzul-Kifli[1], Mohd Mustafa Awang Kechik[1,*], Chen Soo Kien[1,2], Lim Kean Pah[1], Abdul Halim Shaari[1,2], Muhammad Kashfi Shabdin[1], Yazid Yaacob[1], Mohd Hafiz Mohd Zaid[1], Yap Siew Hong[1], Nurhidayah Mohd Hapipi[1]

[1]*Department of Physics, Faculty of Science, Universiti Putra Malaysia, 43400 Serdang, Selangor, Malaysia*
[2]*Institute of Nanoscience and Nanotechnology (ION2), Universiti Putra Malaysia, 43400 UPM Serdang, Selangor, Malaysia*

**Corresponding author (email: mmak@upm.edu.my)*

(Received: 20 November 2025 / Revised: 29 December 2025 / Accepted: 5 January 2026 / Published online: 8 January 2026)

ABSTRACT

The oxygen content in $YBa_2Cu_3O_{7-\delta}$ (YBCO-123) plays a critical role in determining its structural and superconducting properties. In this work, the effect of oxygen flow during the sintering process on the structural, superconducting and microstructural characteristics of pure YBCO-123 was investigated. Samples were prepared using the conventional solid-state reaction method under identical thermal conditions, with and without oxygen flow during sintering. Phase formation and crystal structure were examined using X-ray diffraction (XRD), superconducting behavior was evaluated by AC magnetic susceptibility (ACS) and microstructural features were analyzed using field emission scanning electron microscopy (FESEM). XRD results confirmed that orthorhombic YBCO-123 was the dominant phase for both sintering conditions, with a small amount of Y_2BaCuO_5 (Y-211) secondary phase present. While phase composition differences were minimal, ACS measurement revealed that samples sintered with oxygen flow exhibited a higher superconducting transition temperature and a sharper transition, indicating improved oxygen incorporation and enhanced intergranular coupling. FESEM analysis showed that oxygen-assisted sintering promoted grain growth, improved grain connectivity and reduced porosity. These findings demonstrate that oxygen flow effectively enhances the superconducting and microstructural properties of pure YBCO-123 which highlighting the importance of controlled oxygen environments during thermal processing.

Keywords: AC susceptibility; microstructure; oxygen flow; X-ray diffraction

INTRODUCTION

High-temperature superconductors have attracted considerable attention due to their potential applications in power transmission, magnetic levitation, and electronic devices. Among these materials, $YBa_2Cu_3O_{7-\delta}$ remains one of the most extensively studied superconductors due to its relatively high critical temperature (T_c = 92 K), chemical stability and suitability for large-scale fabrication. Since its discovery by Bednorz and Müller [1], significant efforts have been devoted to understanding the relationship between processing conditions, crystal structure, and superconducting properties of YBCO-123.

The superconducting behavior of YBCO-123 is strongly dependent on its oxygen content, which directly affects charge carrier concentration in the Cu–O chains and CuO_2 planes [2]. The crystal structure of YBCO-123 undergoes a transition from a non-superconducting tetragonal phase to a superconducting orthorhombic phase as oxygen atoms occupy specific lattice sites [3]. Oxygen deficiency, represented by the parameter δ in $YBa_2Cu_3O_{7-\delta}$, leads to lattice distortion, reduced hole concentration and degradation of superconducting properties [4]. Thermal treatment and sintering conditions play a crucial role in determining oxygen stoichiometry and microstructural evolution in YBCO-123. During high-temperature sintering, oxygen diffusion, grain growth and phase formation occur simultaneously. Insufficient oxygen availability during this process can result in oxygen-deficient regions, weak intergranular coupling and reduced superconducting performance [1,5]. Conversely, an oxygen-rich atmosphere can enhance oxygen incorporation into the lattice, stabilize the orthorhombic phase, and improve superconducting properties [2].

In addition to the primary YBCO-123 phase, the formation of a Y_2BaCuO_5 (Y-211) secondary phase has frequently been reported in YBCO systems. This phase is commonly attributed to incomplete peritectic reactions during solidification and cooling [6,7]. While excessive Y-211 content may adversely affect superconductivity, a limited amount of this phase can act as effective flux-pinning centers, potentially enhancing critical current density [3,4]. The formation and distribution of Y-211 are therefore closely linked to processing parameters, particularly sintering temperature and oxygen availability. Although numerous studies have investigated the effects of oxygen annealing on YBCO-123, systematic studies focusing on the role of oxygen flow during the sintering stage itself remain limited, especially for pure, undoped YBCO-123. Understanding how oxygen flow during sintering influences phase formation, oxygen incorporation, microstructure, and superconducting properties is essential for optimizing fabrication routes and improving material performance.

In this work, we investigate the effect of oxygen flow during the sintering process on the structural, superconducting, and microstructural properties of pure YBCO-123. Samples were synthesized under identical thermal conditions, with and without oxygen flow, and characterized using X-ray diffraction (XRD), AC magnetic susceptibility (ACS), and field emission scanning electron microscopy (FESEM). The results provide insight into the role of oxygen-assisted sintering in tailoring the performance of YBCO-123 superconductors.

MATERIALS AND METHODS

Bulk $YBa_2Cu_3O_{7-\delta}$ (YBCO-123) ceramics were synthesized using a thermal treatment method starting from high-purity yttrium(III) nitrate hexahydrate ($Y(NO_3)_3 \cdot 6H_2O$), barium nitrate [$Ba(NO_3)_2$], and copper(II) nitrate hemi-pentahydrate ($Cu(NO_3)_2 \cdot 2.5H_2O$, with polyvinyl pyrrolidone (PVP) employed as a capping agent, following procedures commonly reported for YBCO preparation via solution-based routes [2,8]. All chemicals were purchased from Alfa Aesar (Ward Hill, MA, USA) and used without further purification. The precursor salts and PVP were dissolved in 300 mL of deionized water and magnetically stirred at 80 °C for 2 h to obtain a homogeneous solution. The solution was dried at 110 °C for 24 h, forming a solid gel that was subsequently crushed and ground into a fine powder.

The obtained powder was calcined in two stages at 600 °C for 4 h and 910 °C for 24 h, with intermediate grinding to enhance phase homogeneity. Figure 1 illustrates the schematic mechanism of ion encapsulation by polyvinyl pyrrolidone (PVP) during the synthesis process. During polymerization, the carbon–carbon double bonds (C=C) are disrupted and interact with PVP monomer units, leading to the formation of long polymer chains. The resulting polymer network exhibits resonance characteristics that facilitate the attraction and coordination of metal ions at specific sites within the polymer matrix. As a result, the ions become uniformly dispersed and effectively encapsulated by the PVP chains in the solution. This encapsulation restricts the available space for YBCO particle nucleation, thereby suppressing excessive grain growth and reducing particle agglomeration.

The confined environment created by the PVP matrix further promotes directional and oriented growth of YBCO particles, contributing to enhanced particle stability and microstructural uniformity, as reported in previous studies [8]. During calcination, PVP and other organic components decomposed completely, resulting in the formation of oxide precursors, as reported in previous studies on polymer-assisted synthesis methods [1,9]. After calcination, the powder was reground to ensure uniform particle distribution and then pressed into pellets under a uniaxial pressure of 5 tons. Pellets with diameters of 13 mm and thicknesses of approximately 5 mm were obtained. The pellets were sintered at 980 °C for 24 h in a tubular furnace, either under flowing oxygen or without oxygen flow, to investigate the influence of sintering atmosphere on material properties [6,7].

Phase formation and crystal structure were examined using X-ray diffraction (XRD). Microstructural characteristics were analyzed using scanning electron microscopy (SEM, LEO 1455 VPSEM, Zeiss, Jena, Germany). The superconducting transition temperature (T_c) was determined from AC magnetic susceptibility (ACS) measurements using a lock-in amplifier (SR830) operating at 219 Hz with an applied AC field of 0.5 Oe, a method widely employed for characterizing superconducting transitions in bulk YBCO samples [5,8]. For ACS measurement, the bulk samples were cut into rectangular specimens with dimensions of approximately 5 mm × 2 mm × 1.5 mm.

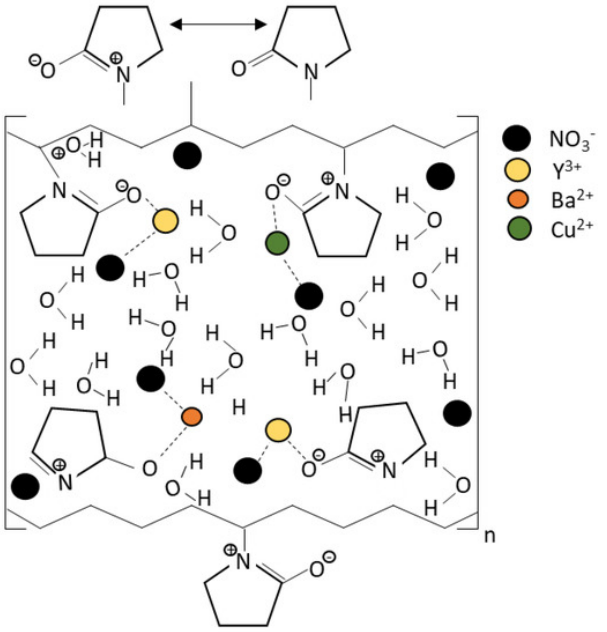


Figure 1. Proposed mechanism of interaction between the PVP and the metal ion [10]

RESULTS AND DISCUSSION

X-ray Diffraction Patterns

Figure 2 shows the X-ray diffraction patterns of pure YBCO-123 samples sintered with oxygen flow and without oxygen flow. For both sintering conditions, the diffraction peaks are predominantly indexed to the YBCO-123 phase. The observed reflections correspond to the orthorhombic crystal structure, which is characteristic of superconducting YBCO materials, in agreement with previous reports on YBCO ceramics prepared by thermal treatment methods [6]. In addition to the dominant YBCO-123 phase, a minor secondary phase corresponding to Y-211 is also detected. The formation of the Y-211 phase has also been reported in other synthesis routes, including the modified thermal decomposition method and thermal treatment methods [11,12]. The Y-211 phase is commonly observed in YBCO systems synthesized at high temperatures and is generally associated with incomplete peritectic reactions during the heat treatment and cooling processes [6,7]. The presence of this phase in both samples suggests that oxygen flow during sintering does not significantly suppress its formation.

Figure 3 presents an enlarged view of the XRD patterns corresponds to the [013] and [103] planes in the 2θ range from 30° to 35°. Two characteristic reflections located at approximately 32.5° and 32.9° are observed for both samples and are indexed to the (013) and (103) planes of the YBCO-123 phase, respectively. The splitting of these peaks is a known feature of the orthorhombic YBCO structure and further confirms the formation of superconducting YBCO-123 [13]. The quantitative phase analysis summarized in Table 1 shows that YBCO-123 remains the dominant phase for both sintering conditions, with only a slight variation in Y-211 content. This indicates that oxygen flow during sintering has a limited influence on phase formation, consistent with previous studies on YBCO ceramics [6].

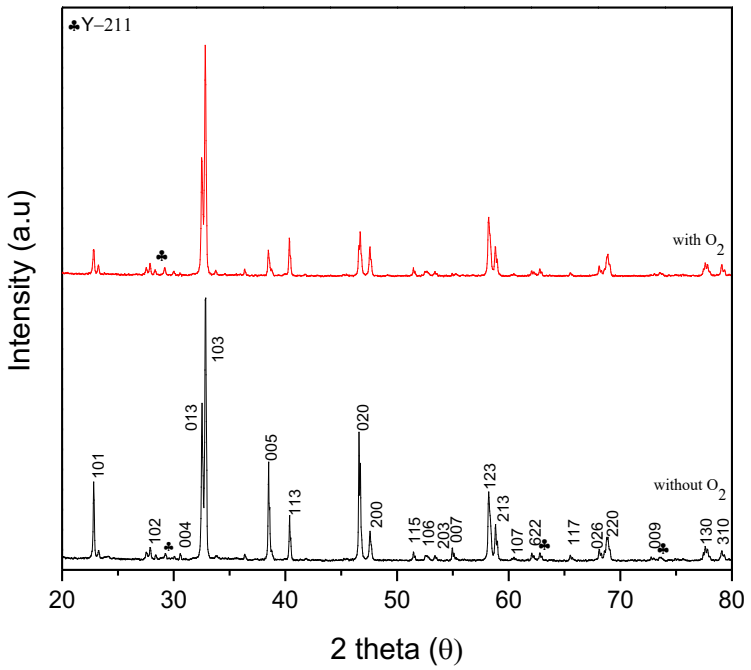


Figure 2. X-ray diffraction patterns of YBCO-123 sintered with oxygen flow and without oxygen flow

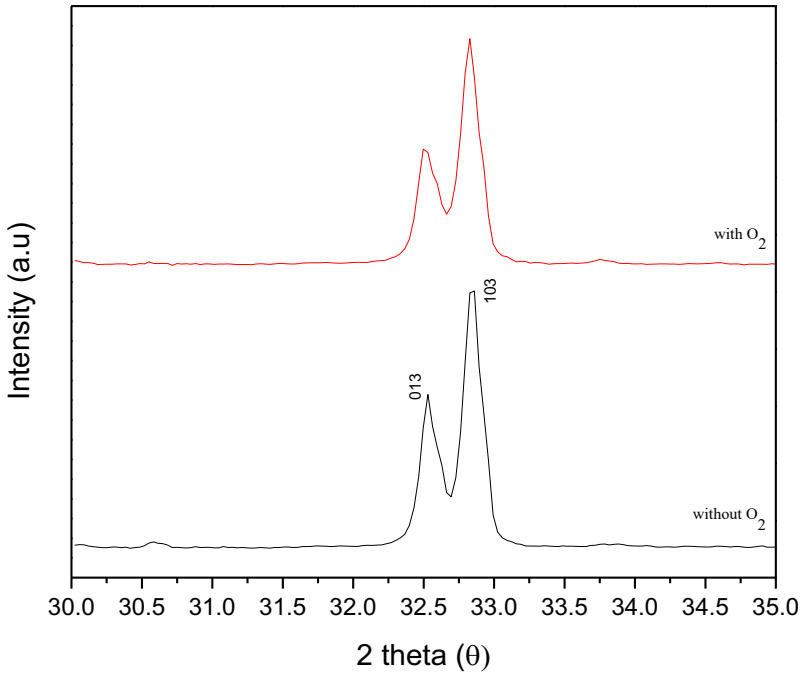


Figure 3. X-ray diffraction pattern corresponds to the [013] and [103] planes of YBCO-123 with oxygen flow and without oxygen flow

Table 1. Different weight percentages of YBCO-123 and Y-211 phases formed for YBCO-123 with and without oxygen flow

YBaCuO	Weight Percentage (%)	
	$YBa_2Cu_3O_7$	Y_2BaCuO_5
without O_2	98.79	1.20
with O_2	97.12	2.88

The crystallite size and lattice parameters derived from XRD analysis are summarized in Table 2. Both samples exhibit lattice parameters (*a*, *b*, and *c*) consistent with the orthorhombic YBCO-123 structure, with no significant variation observed between the two conditions. In contrast, the sample sintered with oxygen flow shows a larger crystallite size, which is consistent with reduced peak broadening and suggests enhanced crystallite growth during sintering [2]. This trend agrees well with the microstructural observations discussed in the FESEM analysis.

Table 2. The summary of crystallite size and lattice parameter *a*-, *b*-, *c*-axis and for YBCO-123 with and without oxygen flow

$YBa_2Cu_3O_{7-\delta}$	Crystallite Size (Å)	Lattice Parameters		
		a (Å)	*b* (Å)	*c* (Å)
without O_2	753	3.819 ± 0.0002	3.886 ± 0.0002	11.682 ± 0.0004
with O_2	1166	3.818 ± 0.0001	3.884 ± 0.0001	11.679 ± 0.0004

Alternating Current Susceptibility (ACS) Analysis

Figure 4 shows the temperature dependence of the AC magnetic susceptibility for pure YBCO-123 samples sintered with oxygen and without oxygen flow. Both samples exhibit a clear superconducting transition, confirming the formation of the superconducting YBCO-123 phase. However, distinct differences in the transition characteristics are observed between the two sintering conditions. The superconducting parameters extracted from the ACS measurement are summarized in Table 3. The sample sintered with oxygen flow shows a higher superconducting transition temperature (T_c) and a sharper transition compared to the sample sintered without oxygen flow, indicating improved superconducting homogeneity and reduced weak-link behavior. Such behavior is consistent with AC susceptibility studies of bulk YBCO, where improved oxygen content enhances carrier concentration and superconducting connectivity [14].

The imaginary component of the ACS signal reveals a coupling peak temperature (T_p), associated with intergranular dissipation and Josephson coupling between grains. As listed in Table 3, the oxygen-flow sample exhibits a higher T_p, indicating stronger intergranular coupling, in agreement with previous reports on oxygen-optimized YBCO ceramics [15]. The higher intergranular critical current density derived from the ACS data further supports improved current transport across grain boundaries for the oxygen-flow sample. The ACS results indicate that oxygen flow during sintering enhances the superconducting performance of pure YBCO-123 by increasing T_c and strengthening intergranular coupling, consistent with the structural and microstructural observations.

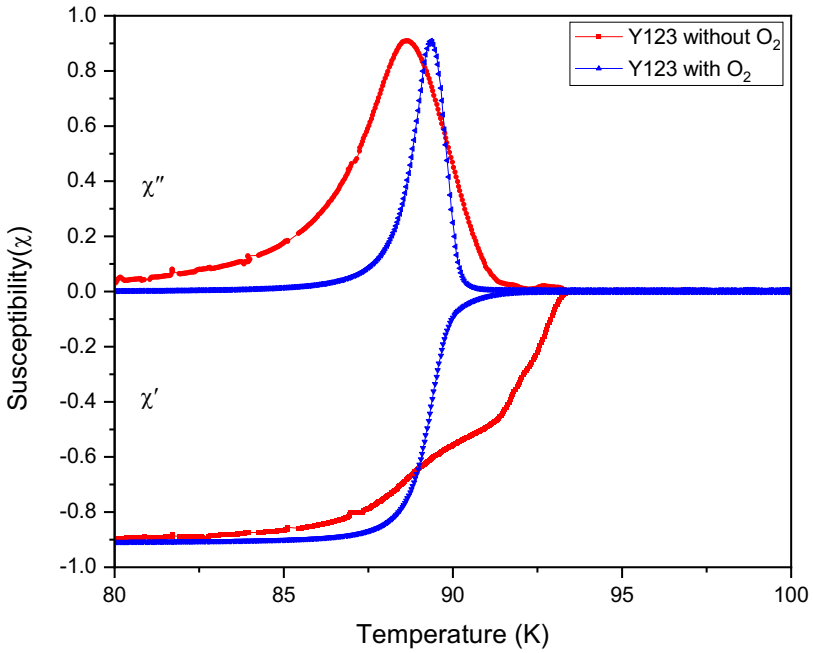


Figure 4. Temperature dependence of the ACS for YBCO-123 sintered with oxygen flow and without oxygen flow, in 0.5 Oe of AC field.

Table 3. Table of the coupling peak temperature (T_p), onset critical temperature (T_c), phase lock-in temperature (T_{cj}) and Josephson current, I_o

YBaCuO	T_p (K)	$T_{c\text{-onset}}$ (K)	T_p / $T_{c\text{-onset}}$	T_{cj} (K)	I_o (mA)	Oxygen Deficiency, δ
without O_2	86.24	88.65	0.97	86.79	0.66	0.09
with O_2	89.91	90.19	0.99	90.09	1.27	0.07

Field Emission Scanning Electron Microscopy (FESEM) Analysis

Figure 5 shows the FESEM micrographs of pure YBCO-123 samples sintered with and without oxygen flow. A clear difference in microstructural features is observed between the two sintering conditions. The sample sintered without oxygen flow exhibits smaller grains with irregular morphology and noticeable porosity, indicating weaker grain connectivity. Similar microstructural characteristics have been reported in YBCO ceramics prepared under limited oxygen conditions, where restricted diffusion leads to incomplete grain growth and poor intergranular contact [4]. In contrast, the sample sintered with oxygen flow shows larger and more uniformly distributed grains with improved grain-to-grain contact and reduced porosity. The denser microstructure suggests enhanced diffusion and grain growth promoted by the presence of oxygen during sintering, which has been shown to improve microstructural homogeneity in YBCO materials [6,7].

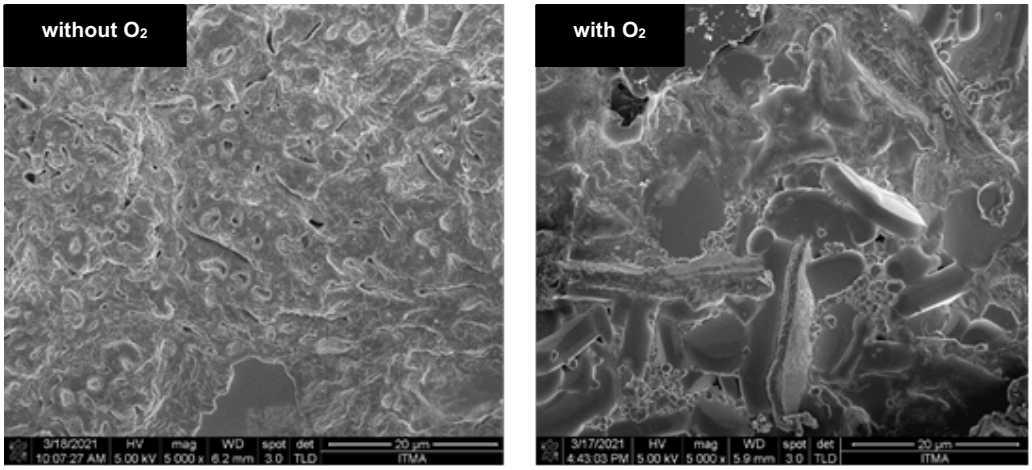


Figure 5. The FESEM micrograph (with 5000× magnification) for the surface YBCO-123 sintered with oxygen flow and without oxygen flow

The average grain size estimated from the FESEM images is summarized in Table 4, where the oxygen-flow sample exhibits a larger grain size (3.934 μm) compared to the sample sintered without oxygen flow (1.844 μm). This observation is consistent with the crystallite size obtained from XRD analysis, indicating good agreement between structural and microstructural results. Improved grain size and connectivity are known to reduce weak-link effects at grain boundaries and enhance intergranular current transport in YBCO superconductors [3]. The FESEM results demonstrate that oxygen flow during sintering significantly improves the microstructural connectivity of pure YBCO-123, which correlates well with the enhanced superconducting properties observed in the ACS measurement.

Table 4. The average size for YBCO-123 sintered with oxygen flow and without oxygen flow

YBaCuO	Average grain size (μm)
without O_2	1.844 ± 0.2
with O_2	3.934 ± 0.6

CONCLUSIONS

The effect of oxygen flow on the structural, superconducting and microstructural properties of pure YBCO-123 during the sintering process has been investigated. XRD analysis confirmed that orthorhombic YBCO-123 is the dominant phase for both sintering conditions, with only a minor Y-211 secondary phase present, indicating that oxygen flow has a limited influence on phase formation. However, AC susceptibility measurements revealed that samples sintered with oxygen flow exhibit a higher superconducting transition temperature and stronger intergranular coupling, reflecting improved oxygen incorporation and superconducting connectivity. FESEM observations further demonstrated that oxygen-assisted sintering promotes grain growth, improves grain

connectivity and reduces porosity. These microstructural improvements are consistent with the enhanced superconducting performance observed in the ACS results. Overall, the findings indicate that controlling oxygen flow during sintering is an effective approach to enhance the superconducting and microstructural properties of pure YBCO-123 without significantly altering its crystal structure.

ACKNOWLEDGMENTS

This research was funded by the Ministry of Higher Education, Malaysia through the Fundamental Research Grant Scheme (FRGS) under project number FRGS 1/2024/STG05/UPM/02/4, grant number FRGS 5540701.

AUTHORS' CONTRIBUTIONS STATEMENT

The manuscript was written through the contributions of all authors. N.A.C.D.-K and Y.S.H designed and organized this work. N.M.H. writing-review and editing. M.M.A.K drafts the main ideas of the work. C.S.K., L.K.P, M.K.S, Y.Y and M.H.M.Z and A.H.S supervising. N.A.C.D.-K. review and editing of the manuscript. All authors have approved the final version of the manuscript.

CONFLICT OF INTEREST

All authors declare no competing interests that could have influenced the work reported in this paper.

REFERENCES

1. Bednorz JG, Müller KA. The discovery of superconductivity above 30 K. *Review of Modern Physics*. 1988;60:585–600.
2. Cava RJ, Hewat AW, Hewat EA, Batlogg B, Marezio M, Rabe K, Krajewski JJ, Peck WF, Rupp LW. Structural anomalies, oxygen ordering and superconductivity in oxygen-deficient $Ba_2YCu_3O_x$. *Physica C*. 1990;165:419–433.
3. Chiang HC, Yang HD, Wu TM. AC susceptibility and intergranular coupling in bulk YBCO superconductors. *Physica C*. 1995;248:231–238.
4. Kim CJ, Hong GW. Defect formation, distribution and size reduction of Y_2BaCuO_5 in melt-processed YBCO superconductors. *Supercondcutor Science and Technology*. 1999;12(3):R27–R42.
5. Ziqq KA. Oxygen content and disorder effects on the critical current density in $YBa_2Cu_3O_x$. *Superconductor Science and Technology*. 2001;14:30.
6. Jorgensen JD, Beno MA, Hinks DG, Soderholm L, Volin KJ, Hitterman RL, Grace JD, Schuller IK. Oxygen ordering and the orthorhombic-to-tetragonal phase transition in $YBa_2Cu_3O_{7-\delta}$. *Physical Review B*. 1987;36:3608–3616.
7. Hassanzadeh-Tabrizi SA, Mazaheri M, Aminzare M, Sadrnezhaad SJ. Reverse precipitation synthesis and characterization of CeO_2 nanopowder. *Journal of Alloys Compounds*. 2010;491:1–7.

8. Singh RK, Varshney D, Khaskalam AJ. Microstructural effects on superconducting properties of $YBa_2Cu_3O_{7-\delta}$ ceramics. *Physica C*. 1998;302:1–8.
9. Rani P, Jha R, Awana VPS. AC susceptibility study of superconducting $YBa_2Cu_3O_{7-\delta}$ bulk composites. *InterCeram: International Ceramic Review.* 2013;68:34–41.
10. Jorgensen JD, Veal BW, Paulikas AP, Nowicki LJ, Crabtree GW, Claus H, Kwok WK. Structural properties of oxygen-deficient $YBa_2Cu_3O_{7-\delta}$. *Physical Review B*. 1990;41:1863–1877.
11. Arebat RAM, Kechik MMA, Kien CS, Pah LK, Baqiah H, Hong YS, Miryala, M. Shaari AH, Zailani TH, Shariff KKM, Shabdin MK, Karim MKA. Influence of oxygen flow vs. ambient annealing on microstructure and superconducting properties of $YBa_2Cu_3O_{7-\delta}$ bulk ceramics. *Journal of Materials Science: Materials in Electronics*. 2025;36(12):760 (p.1-16).
12. Yap SH, Kechik MMA., Humaidi S, Shariff KKM, Baqiah H, Chen SK, Lim KP, Zaid MHM, Yaakob Y, Karim MKA, Talib Z.A, Miryala M. Phase formation, microstructural and superconducting properties of YBCO added Ca-compounds extraction eggshells. *Results in Materials*. 2025;26:100661.
13. Nikolo M. Superconductivity: A guide to alternating current susceptibility measurements and alternating current susceptometer design. *American Journal of Physics*. 1995;63:57–65.
14. Naseri MG, Saion EB, Ahangar HA, Hashim M, Shaari AH. Phase formation and microstructural evolution of $YBa_2Cu_3O_{7-\delta}$ ceramics prepared by thermal treatment method. *Journal of Magnetism and Magnetic Materials*. 2011;323:1745–1750.
15. Chainok P, Khuntak T, Sujinnapram S, Tiyasri S, Wongphakdee W, Kruaehong T, Nilkamjon T, Rateng S, Udomsamuthirun P. Some properties of $YBaCu_{1-x}O_{\gamma}$ superconductors. *Journal of Modern Physics B*. 2015;29:1550060.